

# Electronic transport in single-walled carbon nanotube/graphene junction

Tian Pei,<sup>1</sup> Haitao Xu,<sup>1</sup> Zhiyong Zhang,<sup>1,a)</sup> Zhenxing Wang,<sup>1</sup> Yu Liu,<sup>2</sup> Yan Li,<sup>2</sup> Sheng Wang,<sup>1</sup> and Lian-Mao Peng<sup>1,a)</sup>

<sup>1</sup>Key Laboratory for the Physics and Chemistry of Nanodevices and Department of Electronics, Peking University, Beijing 100871, China

<sup>2</sup>Key Laboratory for the Physics and Chemistry of Nanodevices and College of Chemistry and Molecular Engineering, Peking University, Beijing 100871, China

(Received 30 May 2011; accepted 14 August 2011; published online 12 September 2011)

Graphene/carbon nanotube (CNT) junctions were fabricated by depositing mechanically exfoliated graphene on substrate followed by direct chemical vapor deposition growth of CNT, and their electronic transport properties were investigated. Unlike metallic CNT/graphene junction with good contact, there exists an obvious Schottky barrier between semiconducting CNT and graphene due to the difference of their work functions, which lead to typical rectification properties and directionally field-effect behavior. © 2011 American Institute of Physics. [doi:10.1063/1.3636407]

Low dimension carbon structures, including carbon nanotube (CNT) and graphene, have drawn a lot of attentions in the past 20 years owing to their special physics and chemistry properties and potential applications in many fields.<sup>1,2</sup> Compared to other properties, electronic transport properties of CNT and graphene were under the spotlight since they were regarded as promising alternative building materials for future nanoelectronics.<sup>3–5</sup> Although electronic transport in CNT or graphene had been explicitly explored respectively,<sup>6–8</sup> few investigations had touched on transport through the interface between CNT and graphene,<sup>9</sup> which is an exciting system for exploring carriers transferring between an ideal two-dimensional conductor and an ideal one-dimensional conductor. Moreover, in the terms of applications in electronics, graphene was considered as possible excellent contact electrodes for semiconducting CNT field-effect transistors owing to their “homogeneous” carbon junction.<sup>10,11</sup> Therefore it is essential to investigate and characterize the junction formed between CNT and graphene, which had been seldom explored owing to the difficulty of fabricating such a system. In this letter, we fabricated the CNT/graphene junction through depositing mechanically exfoliated graphene on substrate followed by directly growing ultra-long CNTs on graphene, and the transport properties of the CNT/graphene junction were investigated.

Few-layer graphene samples were derived by mechanical cleavage of Kish graphite and deposited on a heavily n-doped silicon substrate covered with 80 nm thick thermal oxide. Ultra-long CNTs array were directionally grown on SiO<sub>2</sub> substrate via CVD with copper as catalyst and methane as carbon resource,<sup>12</sup> some of the CNTs crossed the pre-deposited graphene forming CNT/graphene junctions. To study electronic transport properties of the junctions, Pd electrodes were fabricated on the other end of CNT or graphene through electron-beam lithography and electron-beam evaporation followed by a standard lift-off process. The schematic diagram of the device is shown in Fig. 1(a) and scanning electron microscopy (SEM) image of a finished

device is shown in Fig. 1(b). In a cryogenic probe station (Lakeshore TTP-4), which is cooled with liquid nitrogen, the electronic measurement was carried out at 77 K in order to reduce outside interference to CNTs including scattering centers from substrate and doped effect from oxygen or aqueous vapor.

Before measuring a CNT/graphene junction, its two main components, i.e., graphene and CNT, were characterized independently. The thickness of graphene is measured by atomic force microscopy (AFM) to be smaller than 10 nm for all junctions in this work, which ensures that the graphite slice is few-layer graphene. To characterize the CNTs, we fabricated a field-effect transistor (FET) near each junction on the same CNT. Field dependent transfer properties of the CNTs were measured by using substrate as back gate, and then we can easily distinguish the nature of the CNT, i.e., a metallic one (m-CNT) or semiconducting one (s-CNT). The transport properties of CNT/graphene junctions were then measured, and two typical electrical characteristics were observed as shown in Fig. 1(c). The dotted curve in the figure corresponds to m-CNT/graphene junction, and the solid line indicates s-CNT/graphene. In all of the measurements, the Pd electrode contacted to graphene is grounded, and voltage bias is applied on the other Pd electrode contacted to CNT. The m-CNT/graphene junction shows nearly symmetric current-voltage (I-V) characteristic under forward and reverse bias, which is similar to m-CNTs with symmetric metallic contacts.<sup>13</sup> At low bias, the I-V curve of m-CNT/graphene junction is linear with a total resistance about 28 k $\Omega$ , which becomes saturated at high bias. It should be noted that the saturation current of up to 20  $\mu$ A is close to the value limited by optical phonon scattering, i.e., 25  $\mu$ A, suggesting no obvious potential barrier exists between graphene and CNT.<sup>13</sup> We, thus, conclude that graphene can form good contact with metallic CNT.

The situation is very different in the case of s-CNT/graphene junction, which exhibits typical rectification characteristics. As the junction is forward biased, i.e., positive voltage is applied to the CNT, the junction exhibits good conduction with a small threshold voltage of about 0.1 V [see the solid curve in Fig. 1(c)]. When a negative voltage is applied on

<sup>a)</sup> Authors to whom correspondence should be addressed. Electronic addresses: zyzhang@pku.edu.cn and lmpeng@pku.edu.cn.

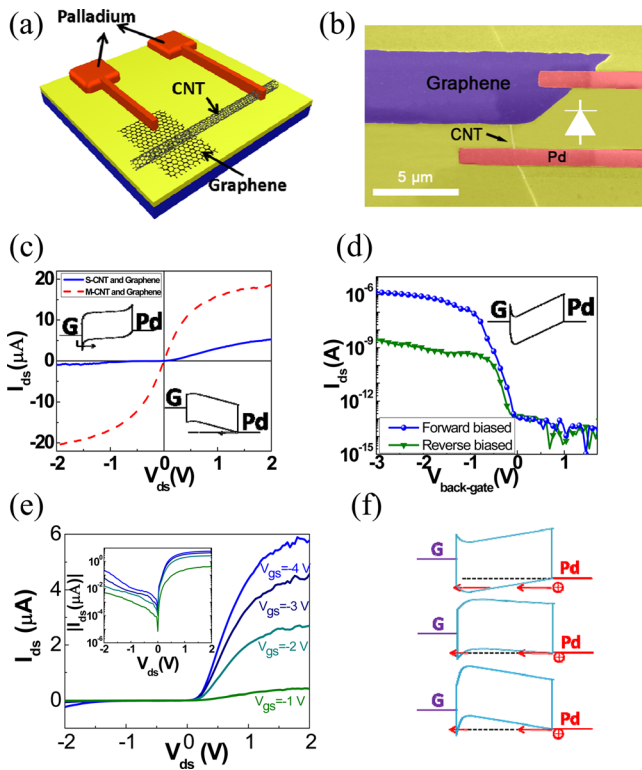


FIG. 1. (Color online) (a) Schematic diagram of CNT/graphene junction device and its (b) SEM image, the scale bar denoting 5  $\mu\text{m}$ . The polarity of this diode is shown in the figure. (c) Comparison of transport characteristics between devices fabricated on an m-CNT and an s-CNT. When measuring the s-CNT/graphene junction, a voltage of  $-3\text{ V}$  is applied at the back gate to tune the CNT to hole accumulation. Inset figures are energy diagram for reverse biased and forward biased device on an s-CNT. (d) Transfer characteristics of this device under forward and reverse bias with  $|V_{ds}| = 0.5\text{ V}$ . Inset figure is energy diagram when the device is turned off by gate voltage. (e) Output characteristics at different gate voltage. Inset figure is output characteristics in logarithmic scale. (f) Energy band diagram of this forward biased device under varying gate voltage. From the upper to lower, this device is gradually turned on by the gate voltage.

CNT, the junction is blocking. The typical rectification characteristic is similar to that of CNT FETs with asymmetric metallic electrodes,<sup>14</sup> suggesting that there exists a Schottky barrier in the system of Pd/s-CNT/graphene/Pd junction. Ohmic contact can be formed between palladium and the conduction band of s-CNT (Ref. 15) so that the contact resistance can be very small. Moreover, according to the properties of m-CNT/graphene junction analyzed previously, no obvious potential barrier formed between graphene and Pd electrode. Therefore, the Schottky barrier must exist between s-CNT and graphene. The rectification characteristics of s-CNT/graphene junction and existence of schottky barrier can also be proved by analyzing energy diagram of such a system. The energy diagrams of the s-CNT/graphene junction under reverse and positive bias are shown in the insets of Fig. 1(c). The Schottky barrier height is determined by the difference between the electron (or hole) affinity of s-CNT and Fermi level of graphene. Since the work function of graphene is about 4.5 eV, which is located to the middle of the band gap of intrinsic s-CNT, there should be a Schottky barrier for both electron and hole with height about  $E_g/2$  ( $E_g$  is the band gap of CNT) between s-CNT and graphene. As the CNT is biased with a negative voltage of  $V_{ds}$ , carriers (here holes) will meet with a barrier with fixed height of  $E_g/2$ , and

then transport through the junction is blocked at low bias. When a positive voltage is biased on CNT, the barrier will be lowered by applied voltage and carriers will pass through the junction easily.

Since the carrier density of a s-CNT and graphene can be simultaneously tuned by back gate, the transport of the s-CNT/graphene junction are thus dependent on gate (silicon substrate) voltage and show typical p-type field-effect as shown in Fig. 1(d). It is obvious that simultaneously considering change of Fermi level both in CNT and graphene is too hard to deal with, and then in our system the effect of Dirac point change with back gate in graphene was neglected owing to two reasons. At first, comparing with the modulation (about several magnitudes) of carriers in s-CNT, the carrier density modulation is much smaller (only several times) in graphene. Second, in our experiment, multiple-layer (generally larger than 3 layers) graphene was used. Since the Dirac point is difficult to be tuned by back gate, there is no need to consider the role of graphene Dirac point, and we only consider the carrier density modulated by back gate in s-CNT. When a positive voltage is applied on the gate, the CNT is electron accumulated. The barrier between CNT and Pd electrode is very large for electron as shown in the inset of Fig. 1(d), and then the s-CNT/graphene device is completely closed to current lower than  $10^{-13}\text{ A}$  whenever positive or negative bias on graphene. As the gate is biased with a negative voltage, hole is accumulated in the CNT and becomes the majority carrier in the device. Since the barrier between CNT and Pd electrode is very small for hole, the barrier at s-CNT/graphene junction begins to dominate the transport properties of the devices. It is obvious that the p-type field-effect behavior is originated from the Pd contact to s-CNT. If Sc or Y is used as the contact electrode of CNT instead of Pd, the s-CNT/graphene junction will show n-type behavior since hole will be blocked at the Sc/CNT interface.<sup>16–18</sup> In its p-type branch, the device is a directionally dependent field-effect transistor<sup>14</sup> owing to the Schottky barrier at the s-CNT/graphene junction, which leads to a current under forward bias about 100 times larger than that under reverse bias. The on/off ratio of the device is up to about  $10^7$  at forward bias, while it is as low as about  $10^5$  at reverse bias. The output characteristics at different gate voltages are shown in Fig. 1(e), which further indicates the devices are directionally FET. At reverse bias, the barrier of s-CNT/graphene junction becomes thinner as increasing negative gate voltage, and then current will increase owing to tunneling. At forward bias, the current also increases with negative gate voltage owing to combination of thinning forward barrier and increasing hole density, which can be explained by the energy diagram in Fig. 1(f). When the energy band bends upward by increasing negative gate voltage, the barrier between CNT and graphene becomes thinner so that the transmission probability is higher. Thus the current will increase with negative gate voltage, no matter the device is reverse biased or forward biased. It should be noted the s-CNT/graphene junction is a good diode with rectification ratio larger than 100 under various negative gate voltages.

To explore the possibility of using graphene as contacts for s-CNT devices, we fabricated a CNT FET with graphene as S/D electrodes as shown in Fig. 2(a). As shown in Fig. 2(b), the I-V curve is almost symmetric under forward and

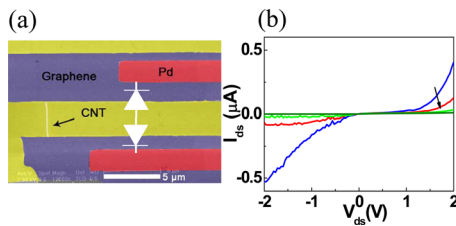


FIG. 2. (Color online) (a) SEM image of a device with graphene as S/D contacts. It can be viewed as two back-to-back diodes. (b) Output characteristics of the device in (a).

reverse bias due to symmetric S/D contacts, but the value of current is much smaller than that of CNT FETs with ohmic contact.<sup>14–18</sup> Considering the barrier between graphene and CNT discussed above, this device comprises two Schottky barrier contacted back-to-back.<sup>19</sup> There must be a reverse biased Schottky barrier to block the pass of carriers regardless of flow direction, and the current is thus seriously reduced to smaller than  $0.5 \mu\text{A}$  which is of the same magnitude as the current of published CNT FETs with graphene contacts.<sup>10,11</sup> Therefore graphene is not a good choice as contact electrodes for semiconducting CNT-based transistors.

In conclusion, CNT/graphene junctions were fabricated by depositing graphene on substrate followed by CVD growing CNTs, and the electronic transport properties were measured. It was found that there exists no obvious Schottky barrier at metallic CNT/graphene junction and graphene is a good contact material for m-CNTs, but a Schottky barrier exists between s-CNT and graphene due to the difference in their work functions, leading to a typical rectification properties and directionally field-effect behavior. Because of the Schottky barrier between graphene and CNT, graphene is not good contact electrodes for CNT FET.

This work was supported by the Ministry of Science and Technology of China (Grant Nos. 2011CB933001 and 2011CB933002), the Fundamental Research Funds for the Central Universities, and National Science Foundation of China (Grant Nos. 61071013 and 61001016).

- <sup>1</sup>R. H. Baughman, A. A. Zakhidov, and W. A. de Heer, *Science* **297**, 787 (2002).
- <sup>2</sup>A. K. Geim, *Science* **324**, 1530 (2009).
- <sup>3</sup>P. Avouris, Z. H. Chen, and V. Perebeinos, *Nat. Nanotechnol.* **2**, 605 (2007).
- <sup>4</sup>F. Schwierz, *Nat. Nanotechnol.* **5**, 487 (2010).
- <sup>5</sup>M. Burghard, H. Klauk, and K. Kern, *Adv. Mater.* **21**, 2586 (2009).
- <sup>6</sup>M. J. Biercuk, S. Ilani, C. M. Marcus, and P. L. McEuen, *Carbon Nanotubes* **111**, 455 (2008).
- <sup>7</sup>J.-C. Charlier, X. Blase, and S. Roche, *Rev. Mod. Phys.* **79**, 677 (2007).
- <sup>8</sup>A. H. C. Neto, F. Guinea, N. Peres, K. S. Novoselov, and A. K. Geim, *Rev. Mod. Phys.* **81**, 109 (2009).
- <sup>9</sup>S. Paulson, A. Helder, M. B. Nardelli, R. M. Taylor II, E. Falvo, R. Superfine, and S. Washburn, *Science* **290**, 1742 (2000).
- <sup>10</sup>B. Li, X. Cao, H. G. Ong, J. W. Cheah, X. Zhou, Z. Yin, H. Li, J. Wang, F. Boey, W. Huang, and H. Zhang, *Adv. Mater.* **22**, 3058 (2010).
- <sup>11</sup>S. Jang, H. Jang, Y. Lee, D. Suh, S. Baik, B. H. Hong, and J.-H. Ahn, *Nanotechnology* **21**, 425201 (2010).
- <sup>12</sup>W. W. Zhou, Z. Y. Han, J. Y. Wang, Y. Zhang, Z. Jin, X. Sun, Y. W. Zhang, C. H. Yan, and Y. Li, *Nano Lett.* **6**, 2987 (2006).
- <sup>13</sup>Z. Yao, C. L. Kane, and C. Dekker, *Phys. Rev. Lett.* **84**, 2941 (2000).
- <sup>14</sup>M. H. Yang, K. B. K. Teo, W. I. Milne, and D. G. Hasko, *Appl. Phys. Lett.* **87**, 253116 (2005).
- <sup>15</sup>A. Javey, J. Guo, Q. Wang, M. Lundstrom, and H. J. Dai, *Nature* **424**, 654 (2003).
- <sup>16</sup>Z. Y. Zhang, X. L. Liang, S. Wang, K. Yao, Y. F. Hu, Y. Z. Zhu, Q. Chen, W. W. Zhou, Y. Li, Y. G. Yao, J. Zhang, and L.-M. Peng, *Nano Lett.* **7**, 3603 (2007).
- <sup>17</sup>Z. Y. Zhang, S. Wang, L. Ding, X. L. Liang, T. Pei, J. Shen, H. L. Xu, Q. Chen, R. L. Cui, Y. Li, and L.-M. Peng, *Nano Lett.* **8**, 3696 (2008).
- <sup>18</sup>L. Ding, S. Wang, Z. Y. Zhang, Q. S. Zheng, Z. X. Wang, T. Pei, L. J. Yang, X. L. Liang, J. Shen, Q. Chen, R. L. Cui, Y. Li, and L.-M. Peng, *Nano Lett.* **9**, 4209 (2009).
- <sup>19</sup>Z. Y. Zhang, C. H. Jin, X. L. Liang, Q. Chen, and L.-M. Peng, *Appl. Phys. Lett.* **88**, 073102 (2006).